Chapter-4

NONLINEAR FLUCTUATIONS IN GRAVITATING POLYTROPIC CHARGED DUST CLOUDS

Abstract: *We study the evolutionary dynamics of weakly nonlinear gravito-electrostatic fluctuations in a self-gravitating polytropic dust molecular cloud in quasi-hydrostatic equilibrium configuration*[†]*. It is a nonthermalized situation in the constituent cold dust grain dynamics; but, mutually thermalized in the dynamics of constituent hot electrons and hot ions. It is specifically demonstrated that the cloud fluctuation dynamics is governed by a new gravito-electrostatically coupled pair of the modified Korteweg-de Vries (m-KdV) equations having unique self-consistent nonlinear sources. A numerical illustrative shape-analysis shows that solitary wave spectral patterns, both compressive (gravitational) and rarefactive (electrostatic), are indeed excitable in the cloud. The electrostatic waves show bi-periodicity, while, the self-gravitational ones retain uni-periodicity in the defined potential phase space.*

4.1 INTRODUCTION

Nonlinear waves in multispecies self-gravitating dusty plasmas have been an important area of research investigation because of their roles in the formation processes of diverse galactic structures, such as stars, planets, nebulae, cometary comae and tails, and other astrophysical structures [1-3]. The evolution of such waves in the nonlinear regime is usually governed by the Korteweg-de Vries (KdV) type of equations, or by their derivative forms, due to the convective nonlinearity and linear dispersion of the media [3]. It has later been predicted analytically that the dust acoustic waves and oscillations propagating through a polytropic dust molecular cloud is governed by an extended KdV (*e*-KdV) equation having a linear integral source arising due to the gravitational interaction of the heavier dust grains [3].

In addition to the above, various dynamical aspects of linear and nonlinear plasma waves in dusty space and astrophysical plasmas have been reported [3-6], like solitary waves,

[†]Gohain, M. and Karmakar, P. K. Gravito-electrostatic fluctuations of a polytropic charge dust cloud. *Physica Scripta*, 89:125604(1-12), 2014.

shock waves, double layers, vortices, voids, etc. These diverse eigen-mode structures have been predicted to result from a complex interplay of nonlinearity, dispersion, dissipation, and so on. In the strong nonlinear regime, the Sagdeev potential approach has been adopted to investigate the properties of both rarefactive and compressive solitary spectral patterns for varieties of dust species [7-10]. It may be noted that the Sagdeev potential approach (strongly nonlinear non-perturbative technique) is validated for any arbitrary amplitude of the fluctuations against the multiple scaling techniques (reductive perturbation techniques) meant for weakly nonlinear fluctuations. The later techniques have been applied methodologically to study the stability behaviors of diverse astrophysical dust clouds resulting in a plethora of miscellaneous solitary, shock-like and hybrid spectral patterns amid inhomogeneous gravity on the Jeans scales of space and time [11-14]. Nevertheless, none has so far investigated the excitation dynamics of nonlinear eigen-mode patterns in a polytropic complex dusty plasma configuration in the presence of nonlocal long-range gravitational interactions in detail.

In this chapter, we propose a theoretical model to study the weakly nonlinear behavior of gravito-electrostatic wave fluctuations in a polytropic self-gravitating dusty plasma system in field-free hydrodynamic equilibrium configuration on the astrophysical scales of space and time. The plasma constituents are the lighter electrons, less light singly ionized positive ions, heavier inertial spherical micron-sized dust grains with full ionization. The massive dust-grain dynamics adopted is such that the first-order self-gravity becomes significant amid diverse spatiotemporal plasma inhomogeneties normally neglected for analytical simplification. The analytical infrastructure is developed by applying a standard multi-scale analysis [11-14] to derive a new gravito-electrostatically coupled pair of the modified KdV (*m*-KdV) equations involving self-consistent nonlinear sources. The source terms arise due to diverse gravito-electrostatic inhomogeneities thereby driving the fluctuations. A detailed numerical illustrative shape-analysis exhibits the excitations of both compressive (gravitational) and rarefactive (electrostatic) solitary spectral patterns. Their relevant properties, like fields, scale-lengths, curvatures and geometrical trajectories are also investigated. It is interestingly found that the electrostatic fluctuations undergo bi-periodicity, while the self-gravitational counter parts retain uni-periodicity in our defined phase space.

4.2 PHYSICAL MODEL

We consider an unmagnetized polytropic configuration of a one-dimensional (1-D) charged dust molecular cloud in a quasi-hydrostatic equilibrium. The hydrostatic equilibrium of the self-gravitating multispecies dusty cloud consists of the lighter electrons, less light ions and heavier charged dust grains. The justification behind adopting the polytropic dust cloud is that the simplest way of allowing spatial variation of the temperature in an astrophysical configuration is to replace the isothermal assumption by a polytropic energy equation involving pressure and density fields in accordance with the universal law of conservation of energy [15]. The constitutive collective dynamics is assumed to maintain a presumed global quasi-neutrality condition. The mathematical simplicity of the model ignores the grain-size distribution, grain-mass distribution, equilibrium spatiotemporal inhomogeneities, rotational dynamics of the grains, etc. The multi-fluidic polytropic cloud system is finally closed with the coupling classical electro-gravitational Poisson equations for potential distributions created by the charge and matter density fields. Such polytropic situations are indeed realizable in many star-forming molecular clouds, stellar atmospheres and accretion disks.

4.3 MATHEMATICAL FORMULATION

The equilibrium dynamics of the self-gravitating charged dust molecular cloud in polytropic configuration, as already mentioned above, is dictated by a closed set of normal fluid equations involving the continuity equation, momentum equation, polytropic equation of state and closing Poisson equations for electro-gravitational potential distributions. Before presenting the fluid formalism, the adopted normalization scheme is shown in Table 4.1.

Table 4.1: Details of normalization scheme

S No.	Physical parameters	Normalizing parameters
1	Position (ξ)	Jeans length (λ_J)
2	Time (τ)	Jeans time (ω_J^{-1})
3	Population density (N_s)	Equilibrium population density (n_{s0})
4	Flow velocity (M_s)	Acoustic phase speed (c_S)
5	Thermal pressure (P_s)	Equilibrium thermal pressure (p_{s0})
6	Electrostatic potential (Φ)	Effective electron thermal potential (T_s/q_s , with s=e)
7	Gravitational potential (Ψ)	Same (T_s/q_s , with s=e)

Here, the suffix '*s*' characterizes the type of the different plasma constituents (electrons, ions and charged dust grains). Thus, the basic set of the normalized equations [3] governing such a cloud in a spatially-flat coordination space defined by (*x*, *t*) is enlisted as follows,

$$\frac{\partial N_s}{\partial \tau}+\frac{\partial}{\partial \xi}\left(N_s M_s\right)=0\,, \tag{4.1}$$

$$\frac{\partial M_s}{\partial \tau}+M_s\frac{\partial M_s}{\partial \xi}+\frac{q_s}{m_s}\frac{\partial \Phi}{\partial \xi}+\frac{\partial \Psi}{\partial \xi}=-\frac{1}{N_s m_s}\frac{\partial P_s}{\partial \xi}\left[\frac{p_{s0}}{n_{s0}\lambda_J}\right], \tag{4.2}$$

$$P_s=C_s N_s^{\gamma_s}\left[\frac{n_{s0}^{\gamma_s}}{p_{s0}}\right]. \tag{4.3}$$

The closing normalized Poisson equations for electrostatic and self-gravitational potentials are respectively given by

$$\in_0 \frac{\partial^2 \Phi}{\partial \xi^2}=-\sum_s N_s q_s\left[\frac{n_{s0}q_s\lambda_J^2}{T_s}\right], \tag{4.4}$$

$$\frac{\partial^2 \Psi}{\partial \xi^2}=4\pi G\sum_s N_s m_s\left[\frac{n_{s0}q_s\lambda_J^2}{T_s}\right]. \tag{4.5}$$

The notation ξ represents the normalized position coordinate, τ the normalized time, N_s the normalized plasma density corresponding to the plasma species characterized by '*s*', M_s the normalized acoustic phase speed described by the label *s*, P_s the normalized pressure corresponding to the label *s* of the species with temperature T_s (in eV), Φ the normalized electrostatic potential and Ψ the normalized self-gravitational potential. Both ϕ and ψ are each normalized by the electron thermal potential (T_s/q_s, with *s*=*e*) for a common comparison with the same equivalence standpoint.

For a standard scale-invariant analysis, we now apply a standard normalization technique of astrophysical significance [11-13]. It may be pertinent to add that the self-gravitating plasmas are indeed inhomogeneous in nature due to large-scale gradient dynamics [16-20]. So, all the characteristic equilibrium parametric values keep on spatiotemporally changing from point to point [16-19]. Thus, adopting constant normalization parametric values, which are dependent on the diverse plasma equilibrium variables throughout the entire cloud, is not so justifiable in such realistic non-uniform situations [17-19]. But, within

the framework of the Jeans homogenization assumption (Jeans swindle) of self-gravitating inhomogeneous medium thereby validating local analyses [20], our choice of the normalization constants dependent of the equilibrium parameter values is well justified for analytical simplification leading to a nonlinear normal (local) mode analysis.

We, with all the salient reservations, now assume that the perturbations of our interest are local, meaning that their wavelengths are much smaller than the relevant inhomogeneity scale lengths. Accordingly, the relevant dependent variables (F) appearing in equations (4.1)-(4.5) are now expanded nonlinearly (in $\in$-powers) around the respective homogeneous equilibrium values (F_0) under weak nonlinearity approximation (perturbation order $\alpha < 3$) as

$$F = F_0 + \sum_{\alpha=1}^{\infty} \in^{\alpha} F_{\alpha}, \tag{4.6}$$

where, $F = \left[N_s \;\; P_s \;\; M_s \;\; \Phi \;\; \Psi\right]^T$, (4.7)

$$F_0 = \left[1 \;\; 1 \;\; 0 \;\; 0 \;\; 0\right]^T, \tag{4.8}$$

$$F_{\alpha} = \left[N_{s\alpha} \;\; P_{s\alpha} \;\; M_{s\alpha} \;\; \Phi_{\alpha} \;\; \Psi_{\alpha}\right]^T. \tag{4.9}$$

4.4 Coupled *m*-KdV equations

The nonlinear fluctuation dynamics in the considered polytropic astrofluid is already mentioned as being governed by a coupled pair of the *m*-KdV equations. For deriving the *m*-KdV system, we introduce slow stretched variables [11-14] for space and time as

$$X = \in^{1/2} (\xi - \mu\tau),\; T = \in^{3/2} \tau, \tag{4.10}$$

where, $\in$ is a smallness parameter measuring the balanced strength of the nonlinearity and dispersion, and μ is the normalized phase velocity of the reference frame. It transforms the spatiotemporal linear differential operators as $\partial/\partial\xi = \in^{1/2} \partial/\partial X$, $\partial^2/\partial\xi^2 = \in \partial^2/\partial X^2$ and $\partial/\partial\tau = \in^{3/2} \partial/\partial T - \mu \in^{1/2} \partial/\partial X$. We now use equations (4.6) and (4.10) in equations (4.1)-(4.5). Equating the like terms (in powers of $\in$) from both sides of equation (4.1), one gets

$$\in^{3/2}: -\mu \frac{\partial N_{s1}}{\partial X} + \frac{\partial M_{s1}}{\partial X} = 0, \tag{4.11}$$

$$\in^{5/2}: \frac{\partial N_{s1}}{\partial T} - \mu \frac{\partial N_{s2}}{\partial X} + \frac{\partial M_{s2}}{\partial X} + \frac{\partial \left(N_{s1} M_{s1}\right)}{\partial X} = 0, \tag{4.12}$$

$$\in^{7/2}: \frac{\partial N_{s2}}{\partial T} + \frac{\partial \left(N_{s1} M_{s2}\right)}{\partial X} + \frac{\partial \left(N_{s2} M_{s1}\right)}{\partial X} = 0, \tag{4.13}$$

$$\in^{9/2}: \frac{\partial \left(N_{s2} M_{s2}\right)}{\partial X} = 0, \text{ and so forth.} \tag{4.14}$$

Similarly, equating the like terms from both sides of equation (4.2), one gets

$$\in^{3/2}: -\mu \frac{\partial M_{s1}}{\partial X} + \frac{q_s}{m_s} \frac{\partial \Phi_1}{\partial X} + \frac{\partial \Psi_1}{\partial X} = -\frac{1}{m_s} \frac{\partial P_{s1}}{\partial X} \left(\frac{p_{s0}}{n_{s0} \lambda_J} \right), \tag{4.15}$$

$$\in^{5/2}: \frac{\partial M_{s1}}{\partial T} - \mu \frac{\partial M_{s2}}{\partial X} + M_{s1} \frac{\partial M_{s1}}{\partial X} + \frac{q_s}{m_s} \frac{\partial \Phi_2}{\partial X} + \frac{\partial \Psi_2}{\partial X} = -\frac{1}{m_s} \left(\frac{\partial P_{s2}}{\partial X} - N_{s1} \frac{\partial P_{s1}}{\partial X} \right) \left(\frac{p_{s0}}{n_{s0} \lambda_J} \right), \tag{4.16}$$

$$\in^{7/2}: \frac{\partial M_{s2}}{\partial T} + M_{s1} \frac{\partial M_{s2}}{\partial X} = \frac{1}{m_s} \left(N_{s1} \frac{\partial P_{s2}}{\partial X} + N_{s2} \frac{\partial P_{s1}}{\partial X} - N_{s1}^2 \frac{\partial P_{s1}}{\partial X} \right) \left(\frac{p_{s0}}{n_{s0} \lambda_J} \right), \tag{4.17}$$

$$\in^{9/2}: M_{s2} \frac{\partial M_{s2}}{\partial X} = \frac{1}{m_s} \left(N_{s2} \frac{\partial P_{s2}}{\partial X} - N_{s1}^2 \frac{\partial P_{s2}}{\partial X} \right) \left(\frac{p_{s0}}{n_{s0} \lambda_J} \right), \text{ and so on.} \tag{4.18}$$

Similarly, equation (4.3) gives

$$\in^{0}: 1 = C_s \left(\frac{n_{s0}^{\gamma_s}}{p_{s0}} \right), \tag{4.19}$$

$$\in^{1}: P_{s1} = C_s \gamma_s N_{s1} \left(\frac{n_{s0}^{\gamma_s}}{p_{s0}} \right), \tag{4.20}$$

$$\in^{2}: P_{s2} = C_s \gamma_s \left(N_{s2} + \frac{1}{2} \gamma_s N_{s1}^2 - \frac{1}{2} N_{s1}^2 \right) \left(\frac{n_{s0}^{\gamma_s}}{p_{s0}} \right), \text{ and so on.} \tag{4.21}$$

The same order-by-order analysis in various powers of $\in$ from equation (4.4) yields

$$\in^{0}: \sum_s q_s \left(\frac{n_{s0} q_s \lambda_J^2}{T_s \in_0} \right) = 0, \tag{4.22}$$

$$\in^{1}: \sum_s q_s N_{s1} \left(\frac{n_{s0} q_s \lambda_J^2}{T_s \in_0} \right) = 0, \tag{4.23}$$

$$\in^{2}: \frac{\partial^2 \Phi_1}{\partial X^2} + \sum_s q_s N_{s2} \left(\frac{n_{s0} q_s \lambda_J^2}{T_s \in_0} \right) = 0, \tag{4.24}$$

$$\in^3: \frac{\partial^2 \Phi_2}{\partial X^2} = 0, \text{ and so on.} \tag{4.25}$$

Similarly, equation (4.5) yields

$$\in^0: -4\pi G \sum_s m_s \left(\frac{n_{s0} q_s \lambda_J^2}{T_s} \right) = 0, \tag{4.26}$$

$$\in^1: -4\pi G \sum_s N_{s1} m_s \left(\frac{n_{s0} q_s \lambda_J^2}{T_s} \right) = 0, \tag{4.27}$$

$$\in^2: \frac{\partial^2 \Psi_1}{\partial X^2} - 4\pi G \sum_s N_{s2} m_s \left(\frac{n_{s0} q_s \lambda_J^2}{T_s} \right) = 0, \tag{4.28}$$

$$\in^3: \frac{\partial^2 \Psi_2}{\partial X^2} = 0, \text{ and so forth.} \tag{4.29}$$

We apply the customary procedure [15-20] of simplification by replacing the second-order perturbed variables among equations (4.11)-(4.29). Using them in equation (4.24), we get a coupled *m*-KdV equation of unique type for the electrostatic fluctuations presented as

$$A_1 \frac{\partial \Phi_1}{\partial T} + B_1 \Phi_1 \frac{\partial \Phi_1}{\partial X} + \frac{\partial^3 \Phi_1}{\partial X^3} = S_e(X,T), \tag{4.30}$$

where,

$$S_e(X,T) = -C_1 \frac{\partial \Psi_1}{\partial T} - \frac{\partial}{\partial X} \left\{ D_1 \Psi_1 \frac{\partial \Psi_1}{\partial X} + E_1 (\Phi_1 \Psi_1) \right\}, \tag{4.31}$$

which is the self-consistent nonlinear driving source, asymmetric in nature. The different coefficients involved here are given as

$$A_1 = \sum_s \left(\frac{n_{s0} q_s^2 \lambda_J^2}{T_s \in_0} \right) \frac{1}{\mu} \left(\frac{1}{\mu^2 - \frac{1}{m_s} C_s \gamma_s \left(\frac{n_{s0}^{\gamma_s}}{n_{s0} \lambda_j} \right)} \right) \frac{q_s}{m_s}, \tag{4.32}$$

$$B_1 = \sum_s \left(\frac{n_{s0} q_s^2 \lambda_J^2}{T_s \in_0} \right) \left(\frac{2}{\left(\mu^2 - \frac{1}{m_s} C_s \gamma_s \frac{n_{s0}^{\gamma_s}}{n_{s0} \lambda_j} \right)^2} \right) \left(\frac{q_s}{m_s} \right)^2, \tag{4.33}$$

$$C_1 = \sum_s \left(\frac{n_{s0} q_s^2 \lambda_J^2}{T_s \in_0} \right) \frac{1}{\mu} \left(\frac{1}{\mu^2 - \frac{1}{m_s} C_s \gamma_s \left(\frac{n_{s0}^{\gamma_s}}{n_{s0} \lambda_j} \right)} \right), \tag{4.34}$$

$$D_1 = \sum_s \left(\frac{n_{s0} q_s^2 \lambda_J^2}{T_s \in_0} \right) \left(\frac{2}{\left(\mu^2 - \frac{1}{m_s} C_s \gamma_s \frac{n_{s0}^{\gamma_s}}{n_{s0} \lambda_j} \right)^2} \right), \tag{4.35}$$

$$E_1 = \sum_s \left(\frac{n_{s0} q_s^2 \lambda_J^2}{T_s \in_0} \right) \left(\frac{2}{\left(\mu^2 - \frac{1}{m_s} C_s \gamma_s \frac{n_{s0}^{\gamma_s}}{n_{s0} \lambda_j} \right)^2} \right) \frac{q_s}{m_s}. \tag{4.36}$$

Again, we use the same standard method of simplification among the various-order mathematical expressions and terms represented by equations (4.11)-(4.29) in equation (4.28). As a result, the *m*-KdV equation for self-gravitating fluctuations is obtained as

$$A_2 \frac{\partial \Psi_1}{\partial T} + B_2 \Psi_1 \frac{\partial \Psi_1}{\partial X} + \frac{\partial^3 \Psi_1}{\partial X^3} = S_g(X,T), \tag{4.37}$$

where, the self-consistent nonlinear driving source becomes

$$S_g(X,T) = -C_2 \frac{\partial \Phi_1}{\partial T} - \frac{\partial}{\partial X} \left\{ D_2 \Phi_1 \frac{\partial \Phi_1}{\partial X} + E_2 (\Phi_1 \Psi_1) \right\}, \tag{4.38}$$

with the different coefficients involved given as

$$A_2 = -4\pi G \sum_s m_s \left(\frac{n_{s0} q_s \lambda_J^2}{T_s} \right) \frac{1}{\mu} \left(\frac{1}{\mu^2 - \frac{1}{m_s} C_s \gamma_s \left(\frac{n_{s0}^{\gamma_s}}{n_{s0} \lambda_j} \right)} \right), \tag{4.39}$$

$$B_2 = -4\pi G \sum_s m_s \left(\frac{n_{s0} q_s \lambda_J^2}{T_s} \right) \left(\frac{2}{\left(\mu^2 - \frac{1}{m_s} C_s \gamma_s \frac{n_{s0}^{\gamma_s}}{n_{s0} \lambda_j} \right)^2} \right), \tag{4.40}$$

$$C_2 = -4\pi G\sum_s m_s\left(\frac{n_{s0}q_s\lambda_J^2}{T_s}\right)\frac{1}{\mu}\left(\frac{1}{\mu^2-\frac{1}{m_s}C_s\gamma_s\left(\frac{n_{s0}^{\gamma_s}}{n_{s0}\lambda_j}\right)}\right)\frac{q_s}{m_s}, \tag{4.41}$$

$$D_2 = -4\pi G\sum_s m_s\left(\frac{n_{s0}q_s\lambda_J^2}{T_s}\right)\left(\frac{2}{\left(\mu^2-\frac{1}{m_s}C_s\gamma_s\frac{n_{s0}^{\gamma_s}}{n_{s0}\lambda_j}\right)^2}\right)\left(\frac{q_s}{m_s}\right)^2, \tag{4.42}$$

$$E_2 = -4\pi G\sum_s m_s\left(\frac{n_{s0}q_s\lambda_J^2}{T_s}\right)\left(\frac{2}{\left(\mu^2-\frac{1}{m_s}C_s\gamma_s\frac{n_{s0}^{\gamma_s}}{n_{s0}\lambda_j}\right)^2}\right)\frac{q_s}{m_s}. \tag{4.43}$$

We apply a Galilean frame transformation $\rho=(X-T)$ so that $\partial/\partial X=\partial/\partial\rho$ and $\partial/\partial T=-\partial/\partial\rho$. This new reference frame moves with the phase velocity of the fluctuations, where equations (4.30) and (4.37) would be transformed into a time-stationary (ODE) form, respectively, given as

$$-A_1\frac{\partial\Phi_1}{\partial\rho}+B_1\Phi_1\frac{\partial\Phi_1}{\partial\rho}+\frac{\partial^3\Phi_1}{\partial\rho^3}=S_e(\rho), \tag{4.44}$$

where,

$$S_e(\rho)=C_1\frac{\partial\Psi_1}{\partial\rho}-D_1\Psi_1\frac{\partial\Psi_1}{\partial\rho}-E_1\left(\Phi_1\frac{\partial\Psi_1}{\partial\rho}+\Psi_1\frac{\partial\Phi_1}{\partial\rho}\right); \text{ and} \tag{4.45}$$

$$-A_2\frac{\partial\Psi_1}{\partial\rho}+B_2\Psi_1\frac{\partial\Psi_1}{\partial\rho}+\frac{\partial^3\Psi_1}{\partial\rho^3}=S_g(\rho), \tag{4.46}$$

where,

$$S_g(\rho)=C_2\frac{\partial\Phi_1}{\partial\rho}-D_2\Phi_1\frac{\partial\Phi_1}{\partial\rho}-E_2\left(\Phi_1\frac{\partial\Psi_1}{\partial\rho}+\Psi_1\frac{\partial\Phi_1}{\partial\rho}\right). \tag{4.47}$$

Thus, we see that the steady-state form of the fluctuation dynamics of the polytropic cloud is collectively governed by the stationary coupled *m*-KdV system (equations (4.44) and (4.46)). A numerical analysis is needed for exact pattern prediction as presented in the next section.

4.5 RESULTS AND DISCUSSIONS

A theoretical study of gravito-electrostatic fluctuations in a self-gravitating polytropic charged dust molecular cloud is carried out. A coupled pair of *m*-KdV equations governing the fluctuations is derived by applying standard multiple scaling techniques. Interestingly, both the equations are found to involve self-consistent nonlinear sources which depend on the lowest-order gravito-electrostatic potential fluctuations, spatiotemporal inhomogeneities and their interplayed asymmetric coupling. The uniqueness of the derived equations lies in their gradient-driven coefficients evolving in diverse multi-parametric space. So, it is extremely difficult to obtain their exact analytical solutions due to the complicated coupling of diverse spatiotemporal terms in an intermixed form. The model is, consequently, analyzed numerically to display the fluctuation patterns using the well-known fourth-order Runge-Kutta (RK-IV) method [21] for the spatial (stationary) case and finite difference method [22] for the spatiotemporal (non-stationary) case of our interest.

4.5.1 Electrostatic fluctuations

In figure 4.1, we show the spatial profiles of the normalized electrostatic (a) potential (Φ, blue line), field strength ($\partial\Phi/\partial\xi$, red line), potential curvature ($\partial^2\Phi/\partial\xi^2$, green line), and gradient scale length (L_e, black line); and (b) phase portrait (in a phase space defined by Φ and $\partial\Phi/\partial\xi$) to see the geometrical trajectories of the fluctuations. The different input initial values [7-10] used are $\Phi_1 = -1\times10^{-3}$, $\Phi_{1\xi} = -1\times10^{-4}$, $\Phi_{1\xi\xi} = -1\times10^{-5}$, $Z_d = 100$, $G = 6.67\times10^{-11}$ N m^2 kg^{-2}, $\mu = 1$, $\in_0 = 8.854\times10^{-12}$ F m^{-1}, $q_e = -1.6\times10^{-19}$ C, $q_i = 1.6\times10^{-19}$ C, $\gamma = 1.66$, $m_e = 9.1\times10^{-31}$ kg, $m_i = 1.6\times10^{-27}$ kg, $n_{e0} = 2.01\times10^{12}$ m^{-3}, $n_{i0} = 5\times10^{3}$ m^{-3}, $n_{d0} = 2\times10^{-1}$ m^{-3} and $T_e \approx T_i = T_p = 1$ eV.

It is interestingly seen that the electrostatic fluctuations evolve as rarefactive solitonic spectral patterns having two unique compressive tails with relatively smaller wave amplitude [figure 4.1(a)]. The corresponding field variation evolves as an asymmetric admixture of solitons and anti-solitons, growing as bipolar pulse structures, similar to distorted double layers [figure 4.1(a)]. The corresponding potential curvature variation on an average evolves as a compressive solitonic structure having some asymmetric damped periodic rarefactive

tails of anti-solitonic nature [figure 4.1(a)]. The gradient scale length of the potential fluctuations ($L_e = \left[\partial/\partial\xi\left(\log\Phi\right)\right]^{-1}$) shows strong inhomogeneities at about $\xi = 4$ and $\xi = 11$; respectively. It is found that rarefactive sub-solitons with gradually enhancing strengths are formed at this point due to complex interplay of the long-range inter-species interaction forces. The geometrical patterns in our defined phase space show conservative nature of the fluctuations, but with a periodic doubling. Thus, it is seen that the weak electrostatic fluctuations as a whole are conservative in nature.

As in figure 4.2, we portray the spatiotemporal characteristics of the fluctuations, where, the input initial value is taken as $\Phi_0 = \left(\sin\left(\sqrt{x^2+t^2}\right)\right)/\left(\sqrt{x^2+t^2}\right)$ with t=2. The initial value is randomly generated by hit and trial method with the average behavior to go as per the spatial profiles presented before [figures 4.1-4.2]. It is seen that, in the above parameter regime, the electrostatic fluctuations propagate as a periodic wave composed of soliton (compressive) and anti-soliton (rarefactive) patterns. There is, however, no destabilization of the patterns in our defined slow time frame.

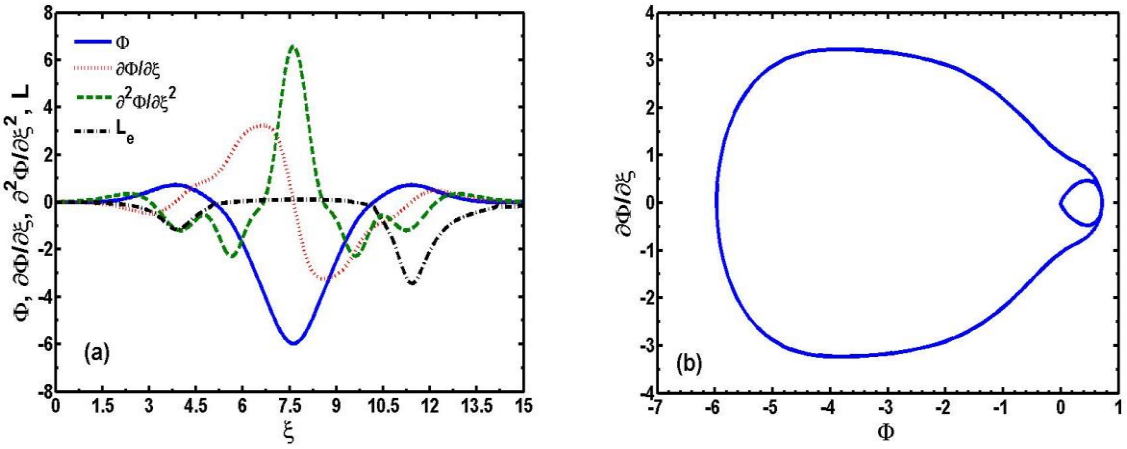

Figure 4.1: *Spatial profile of the normalized electrostatic (a) potential (Φ , blue line), field strength ($\partial\Phi/\partial\xi$, red line), potential curvature ($\partial^2\Phi/\partial\xi^2$, green line), and gradient scale length (L_e , black line); and (b) phase portrait (in a phase space defined by Φ and $\partial\Phi/\partial\xi$). Different input and initial values are given in the text.*

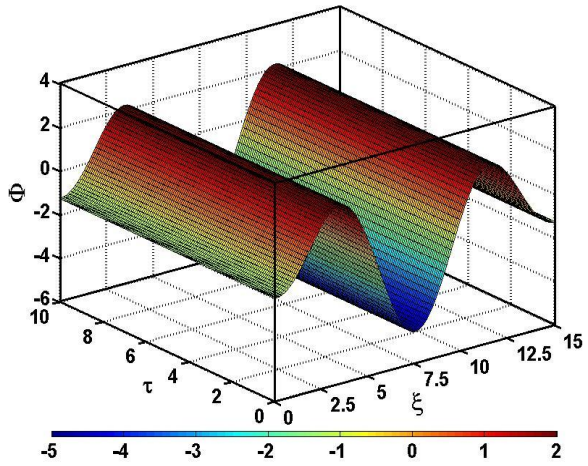

Figure 4.2: *Spatiotemporal profile of the electrostatic potential fluctuations. Input details can be found in the text.*

4.5.2 Self-gravitational fluctuations

The numerical technique as in the electrostatic case is similarly applied to see the exact patterns of the self-gravitational fluctuations. Figure 4.3 represents a spatial profile of the normalized self-gravitational (a) potential (Ψ, blue line), field ($\partial\Psi/\partial\xi$, red line), potential curvature ($\partial^2\Psi/\partial\xi^2$, green line), and gradient scale length (L_g, black line); and (b) phase portrait (in a phase space defined by Ψ and $\partial\Psi/\partial\xi$). The different initial values used are $\Psi_1 = -1\times10^{-1}$, $\Psi_{1\xi} = -1\times10^{-3}$, $\Psi_{1\xi\xi} = 1\times10^{-1}$ and the rest of the input parameters are the same as in the electrostatic case.

From figure 4.3(a), it is observed that the self-gravitational fluctuations evolve as extended compressive solitonic structure. The corresponding field variation [figure 4.3(a)] evolves as a distorted mixture of an anti-soliton (rarefactive) and a soliton (compressive). It shows that a bipolar field (pulse) structure is associated with the soliton. The corresponding potential curvature variation gives the idea that, although the nonlinear fluctuations are weak, the mass-neutrality deviation becomes dominant between $\xi = 6$ and $\xi = 9$. Before and after this range, we get compressive soliton-like structures, but in an aperiodic irregular fashion [figure 4.3(a)]. The scale length ($L_g = \left[\partial/\partial\xi(\log\Psi)\right]^{-1}$) shows strong inhomogeneities at about $\xi = 3$ and $\xi = 12$ relative to the center of the cloud matter mass distribution [figure

4.3(a)]. The conservative nature of the self-gravitational fluctuations is reflected in the phase portrait as shown in figure 4.3(b), and it is found to be uni-periodic parametrically.

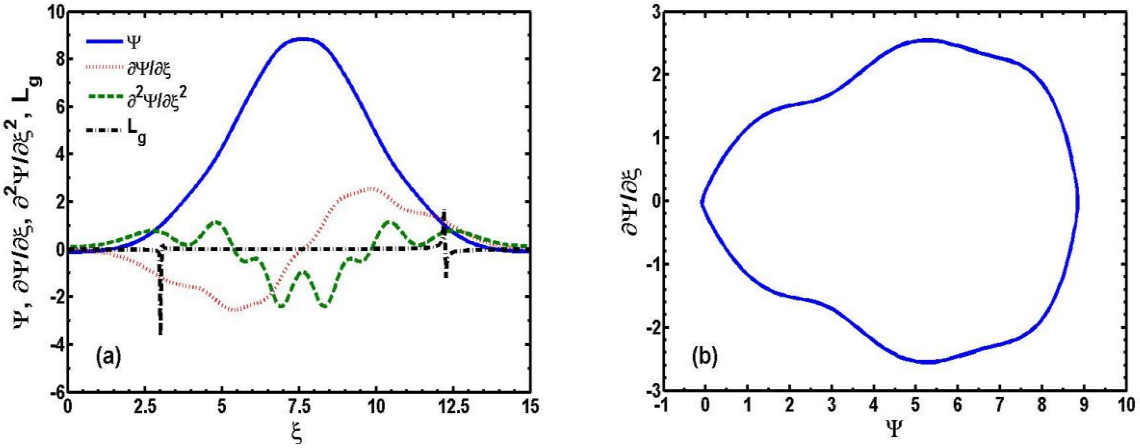

Figure 4.3: *Spatial profile of normalized self-gravitational (a) potential (Ψ , blue line), field strength ($\partial\Psi/\partial\xi$, red line), potential curvature ($\partial^2\Psi/\partial\xi^2$, green line), and gradient scale length (L_g , black line); and (b) phase portrait (in a phase space defined by Ψ and $\partial\Psi/\partial\xi$). Different input and initial values are described in the text.*

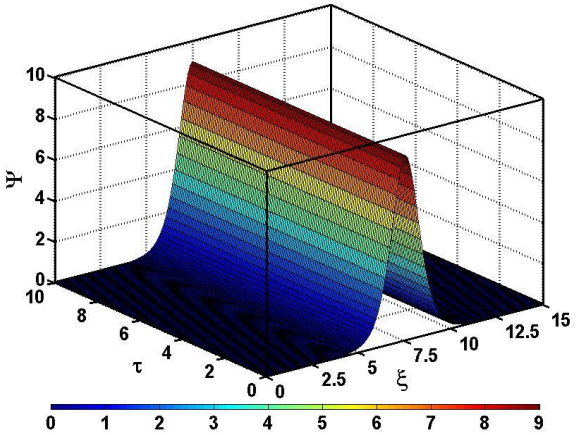

Figure 4.4: *Spatiotemporal profile of self-gravitational potential fluctuation. Different input and initial values used are described in the text.*

4.6 CONCLUSIONS

A methodological study of the nonlinear gravito-electrostatic fluctuations in a self-gravitating polytropic charged dust cloud is carried out. The basic features of nonlinear electrostatic and self-gravitational waves that arise in weakly coupled unmagnetized plasma comprising of the hot electrons, ions; and cold identical charged dust grains is briefly presented. The main conclusive remarks which may be drawn are summarized as the following.

1. The nonlinear eigenmode patterns of a charged polytropic dust cloud dynamically evolve as a new coupled pair of *m*-KdV dynamics with self-consistent nonlinear sources involving coupled gravito-electrostatic interactions in an intermixed form.

2. Numerical shape-analysis shows that electrostatic eigenmodes evolve as rarefactive solitons-like structures (bi-periodic); whereas, the self-gravitational fluctuations evolve as extended compressive solitonic structures (uni-periodic).

3. A detailed numerical analysis of the associated field, curvature and gradient scale length under multi-parameter variation support that both quasi-neutrality and mass-neutrality deviations become maximum at a radial distance 7.5 (on the Jeans scale) relative to the center of the entire cloud mass distribution.

4. The phase space trajectories show the conservative nature of the electrostatic fluctuations with periodic doubling; whereas, the conservative nature of the self-gravitational fluctuations, with a single periodicity is revealed by the geometrical trajectories.

5. The presented solitary spectral patterns of the *m*-KdV dynamics are in partial and qualitative correspondence with the various observations *in situ* made by various spacecraft instrumentations, on-board multispace satellite reports, sophisticated imaging detections and experimental laboratory findings [6, 23]. In addition, molecular clouds well-known to support such structures are *Lynds 204 Complex* [6], *Barnard 68* [23] and so forth.

It is admitted that the entire investigation is based on local analysis valid under the approximation of weak nonlinearity ($<3^{rd}$ order). But, astrophysical analyses would require nonlocal analyses due to diverse equilibrium spatiotemporal inhomogeneities under large scale convective dynamics. Thus, our investigation gives a simplistic picture of the existing eigen-mode patterns in molecular clouds, thereby avoiding such realistic complications.

REFERENCES

[1] Goertz, C. K. Dusty plasmas in the solar system. *Reviews of Geophysics*, 27:271-292, 1989.

[2] Ida, A., Sanuki, H., and Todoroki, J. An extended K-dV equation for nonlinear magnetosonic wave in a multi-ion plasma. *Physica Scripta*, 53:85-88, 1996.

[3] Verheest, F. and Shukla, P. K. Nonlinear waves in multispecies self-gravitating dusty plasmas. *Physica Scripta*, 55:83-85, 1997.

[4] Salahuddin, M. and Shah, H. A. Stability of self gravitating dusty plasma. *Physica Scripta*, 69: 126-130, 2004.

[5] Adams, F. C., Fatuzzo, M., and Watkins, R. Nonlinear waves and solitons in molecular clouds. *Astrophysical Journal*, 403:142-157, 1993.

[6] Watkins, R., Adams, F. C., Fatuzzo, M., and Gehman, C. Nonlinear waves and solitons in molecular clouds. In *Proceedings of the 2nd Cologne-Zermatt Symposium*, Zermatt, Switzerland, Lecture Notes in Physics, edited by Winewisser, G. and Pelz, G. C., volume 459, pages 115-117, 1995, Springer.

[7] Verheest, F. Nonlinear dust-acoustic waves in multispecies dusty plasmas. *Planetary and Space Science*, 40(1):1-6, 1992.

[8] Verheest, F. Waves and instabilities in dusty space plasmas. *Space Science Reviews*, 77(3):267-302, 1996.

[9] Verheest, F. and Yaroshenko, V. V. Nonlinear electrostatic modes in astrophysical plasmas with charged dust distributions. *Astronomy and Astrophysics*, 503:683-690, 2009.

[10] Mamun, A. A. and Shukla, P. K. Electrostatic solitary and shock structures in dusty plasmas. *Physica Scripta*, T98:107-114, 2002.

[11] Karmakar, P. K. Nonlinear stability of pulsational mode of gravitational collapse in self-gravitating hydrostatically bounded dust molecular cloud. *Pramana Journal of Physics*, 76(6):945-956, 2011.

[12] Karmakar, P. K. and Borah, B. New nonlinear eigenmodes of a self-gravitating spherical charged dust molecular cloud. *Physica Scripta*, 86:025503(1-11), 2012.

[13] Karmakar, P. K. and Borah, B. Nonlinear pulsational eigenmodes of a planar collisional dust molecular cloud with grain-charge fluctuation. *European Physical Journal D*, 67:187(1-14), 2013.

[14] Karmakar, P. K. and Borah, B. Inertia-centric stability analysis of a planar uniform dust molecular cloud with weak neutral- charged dust frictional coupling. *Plasma Science and Technology*, 16(5):433-447, 2014.

[15] Chandrasekhar, S. *An Introduction to the Study of Stellar Structure*. Chicago, Illinois, 1939.

[16] Pandey, B. P., Avinash. K., and Dwivedi, C. B. Jeans instability of a dusty plasma. *Physical Review E*, 49(6):5599-5606, 1994.

[17] Cadez, V. M. Applicability problem of Jeans criterion to a stationary self-gravitating cloud. *Astronomy and Astrophysics*, 235: 242-244, 1990.

[18] Vranjes, J. Gravitational instability of a quasi-homogeneous plasma cloud with radiation. *Astrophysics and Space Science*, 173:293-298, 1990.

[19] Verheest, F. and Cadez, V. M. Static configurations of gravitating dusty plasmas. *Physical Review E*, 66:056404(1-7), 2002.

[20] Vranjes, J. Gravitational instability problem of nonuniform media. *Astrophysics and Space Science*, 213(1):139-142, 1994.

[21] Butcher, J. C. An introduction to "Almost Runge-Kutta" methods. *Applied Numerical Mathematics*, 24:331-342, 1997.

[22] Lindfield, G. R. and Penny, J. E. T. *Numerical Methods Using MATLAB*. Elsevier, 2012.

[23] Alves, J. F., Lada, C. J., and Lada, E. A. Internal structure of a cold dark molecular cloud inferred from the extinction of background starlight. *Nature*, 409:159-161, 2001.